IRIS AperTO

UNIVERSITÀ DEGLI STUDI DI TORINO

AperTO - Archivio Istituzionale Open Access dell'Università di Torino

H2O2 direct synthesis under mild conditions on Pd-Au samples: Effect of the morphology and of the composition of the metallic phase

This is the author's manuscript

Original Citation:

Availability:

This version is available http://hdl.handle.net/2318/1564477 since 2017-05-27T12:01:36Z

Published version:

DOI:10.1016/j.cattod.2014.01.015

Terms of use:

Open Access

Anyone can freely access the full text of works made available as "Open Access". Works made available under a Creative Commons license can be used according to the terms and conditions of said license. Use of all other works requires consent of the right holder (author or publisher) if not exempted from copyright protection by the applicable law.

(Article begins on next page)

10 November 2024

IRIS AperTO

UNIVERSITÀ DEGLI STUDI DI TORINO

This Accepted Author Manuscript (AAM) is copyrighted and published by Elsevier. It is posted here by agreement between Elsevier and the University of Turin. Changes resulting from the publishing process - such as editing, corrections, structural formatting, and other quality control mechanisms - may not be reflected in this version of the text. The definitive version of the text was subsequently published in CATALYSIS TODAY, 248, 2015, 10.1016/j.cattod.2014.01.015.

You may download, copy and otherwise use the AAM for non-commercial purposes provided that your license is limited by the following restrictions:

(1) You may use this AAM for non-commercial purposes only under the terms of the CC-BY-NC-ND license.

(2) The integrity of the work and identification of the author, copyright owner, and publisher must be preserved in any copy.

(3) You must attribute this AAM in the following format: Creative Commons BY-NC-ND license (http://creativecommons.org/licenses/by-nc-nd/4.0/deed.en), 10.1016/j.cattod.2014.01.015

The publisher's version is available at:
http://linkinghub.elsevier.com/retrieve/pii/S0920586114000509

When citing, please refer to the published version.

Link to this full text:
http://hdl.handle.net/2318/1564477

This full text was downloaded from iris - AperTO: https://iris.unito.it/

iris - AperTO

University of Turin's Institutional Research Information System and Open Access Institutional Repository

H_2O_2 direct synthesis under mild conditions on Pd-Au samples: effect of the morphology and of the composition of the metallic phase

Federica Menegazzo[a*], Maela Manzoli[b], Michela Signoretto[a], Francesco Pinna[a], Giorgio Strukul[a]

[a]Department of Molecular Sciences and Nanosystems, Ca' Foscari University Venice and Consortium INSTM RU Venice, Dorsoduro 2137, 30123 Venezia, Italy
[b]Department of Chemistry, University of Torino, and NIS Centre of Excellence, via P. Giuria 7, 10125 Torino, Italy

Abstract

Bimetallic Pd-Au samples supported on silica were prepared by different methods and tested for the direct synthesis of hydrogen peroxide under very mild conditions (room temperature and atmospheric pressure), outside the explosion range and without addition of halides. Further catalytic tests were performed at higher pressure using solvents expanded with CO_2. Samples were characterized by N_2 physisorption, metal content analysis, TPR, HRTEM combined with X-Ray EDS probe and DR UV-Vis measurements. The effect of gold addition to Pd in enhancing the yield of H_2O_2 was sensitive to the preparation method: the best catalytic results were obtained introducing gold and palladium by incipient wetness co-impregnation. HRTEM and TPR evidenced the presence of a PdAuO phase able to guarantee the availability of less energetic sites, which activate the oxygen molecule without dissociation. Co-impregnated bimetallic PdAu catalysts on different supports were also tested. The productivity follows the trend: PdAuSi ≈ PdAuSZ > PdAuZ >> PdAuCe ≈ PdAuSCe. The origin of the differences among samples can be due to an effect of the acidity of the support on both morphology and size of the bimetallic phase. HRTEM and DR UV-Vis spectroscopy revealed bimetallic particles exposing the active less energetic sites on PdAuSi, PdAuSZ and PdAuZ, whereas on ceria the presence of more energetic sites that lead to the formation of water were disclosed.

Keywords: hydrogen peroxide direct synthesis; H_2O_2; palladium; gold; bimetallic catalyst; $PdAu/SiO_2$; $PdAu/ZrO_2$; $PdAu/CeO_2$; oxidation

*Corresponding author:
Dr. Federica Menegazzo
Department of Molecular Sciences and Nanosystems
Ca' Foscari University Venice and Consortium INSTM RU Venice,
Dorsoduro 2137, 30123 Venezia, Italy
+390412348552; e-mail fmenegaz@unive.it

Introduction

Hydrogen peroxide is widely accepted as a green oxidant, as it is easy to handle, relatively non-toxic, and breaks down readily to water in the environment [1]. The overall production was 3.52 Mt in 2005 spread over a variety of sectors, among which the fraction going into the production of chemicals is about one fifth of the total market, while the vast majority is consumed by unselective oxidations like the bleaching of textiles, pulp and paper, and in the treatment of wastewaters before they are released into the environment. The continuing replacement of chlorine compounds with hydrogen peroxide in the pulp and paper industry and in environmental applications is expected to drive the production to 4.67 Mt by 2017 [2]. More recent applications in the chemical industry are related to the discovery of TS-1 molecular sieves and their ability to promote large scale selective oxidation processes [3]. These and other possible smaller scale applications of hydrogen peroxide would greatly benefit from on-site, moderate scale production facilities capable of reducing costs. In fact, for hydrogen peroxide to successfully break into new markets the production should become less expensive. Presently the anthraquinone route (AO) [2, 4] is almost the only process used worldwide, with more than 90% share. This process, although practised on a multi-million ton scale annually, suffers from several limitations:

(i) a significant amount of organic waste due to the over-reduction of anthraquinone;
(ii) low conversion during the hydrogenation step in order to minimize secondary reactions;
(iii) difficulties in the complete recovery of the hydrogenation catalyst;
(iv) the need of several energy consuming separation and concentration steps;
(v) the use benzene as the solvent;
(vi) an economic feasibility only on large scale plants.

The development of a new, more economic process to synthesize H_2O_2 is considered a key step towards the introduction of new selective oxidation processes for sustainable production [2]. The direct synthesis of H_2O_2 from H_2 and O_2 is a possible way towards small scale plants that may potentially half the cost of hydrogen peroxide with respect to the commercial process [5]. The environmental impact of the direct route would be lower than in the current commercial route. Clearly, the contact between H_2 and O_2 is a significant safety hazard while operation under intrinsically safe conditions is very important for the viability of the process. In addition, another major problem associated with the process is the generally low H_2O_2 selectivity. Hydrogen peroxide is unstable with respect to both hydrogenation and radical decomposition, and the most thermodynamically favored reaction between hydrogen and oxygen is, by far, water formation, as shown in Scheme 1.

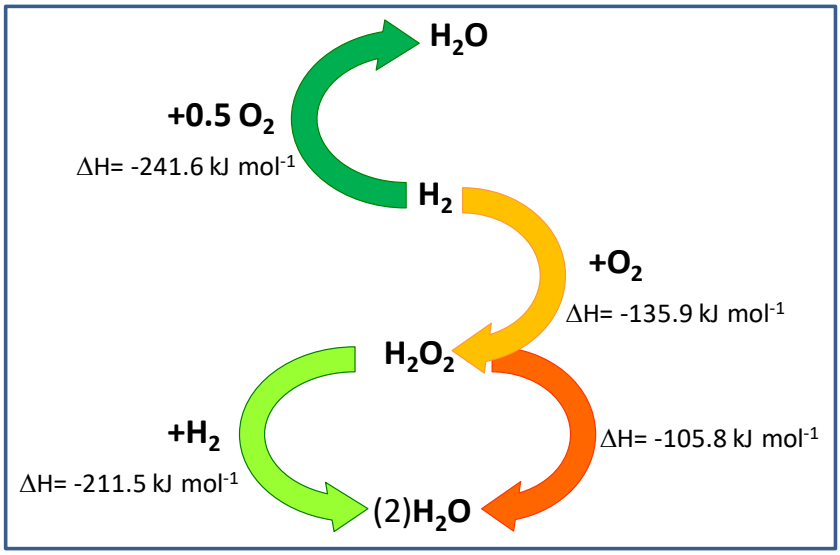

Scheme 1.

Therefore, in spite of several published patents [4-11] and recent literature [12-22], at present no process for the direct synthesis of hydrogen peroxide has yet found the way to commercialization. Still open challenges are the need to operate under intrinsically safe conditions with both an adequate selectivity towards the desired reaction and a hydrogen peroxide productivity that could be of practical significance (at least 1–2% solutions).

In this respect an important role is played by the support and its capacity to impart the appropriate metal morphology.

Many different supports have been investigated for this reaction, but the most common ones are silica [23] and charcoal [24]. We have recently performed a comparison among monometallic palladium based samples over different supports. In a semibatch reactor under mild conditions Pd/SiO_2 gives the highest selectivity and productivity [25], while catalysts supported on sulphated zirconia and ceria performed better by continuous operation in a trickle bed reactor [26]. On the other hand Edwards et al. have found that PdAu carbon–supported catalysts give the highest reactivity, while PdAu samples on TiO_2 and SiO_2 performed better than that on Al_2O_3 and Fe_2O_3 [16] under the same experimental conditions. So far Pd has qualified as the best catalytic material [27-29]. However, it is well known that alloying or combining two metals can lead to materials with specific chemical properties due to an interplay of “ensemble” and “electronic” effects [30], and that a bimetallic surface can exhibit catalytic properties that are very different from those of the surfaces of the individual metals. It has also been demonstrated that the combination of Pd with Au [31-33], Ir [34], Ag [35], and Pt [31, 35-37] can improve both the productivity and the selectivity of the process. As far as gold is concerned, since the pioneering work of Haruta et al. [38], gold

nanoparticles supported on metal oxides have been known to be active in some important industrial reactions [39-42], the present reaction being not included. We have already demonstrated [33, 43] for both plain and sulphated zirconia and ceria supports, that while the monometallic gold catalysts are inactive under mild experimental conditions, the addition a 1:1 amount of gold to a monometallic Pd sample improves the productivity and especially the selectivity of the process. In these samples gold must be in close contact with Pd, as its presence profoundly changes Pd dispersion as well as its morphology and charge. However, no evidence for small Au particles was ever found, probably because of the preparation conditions.

In the present work we report the synthesis by different methods of Pd-Au samples supported on silica. They have been tested in the direct synthesis of hydrogen peroxide both under very mild conditions (1 bar and 20 °C and outside the explosion range) and at higher pressure (10 bar) using solvents expanded with CO_2 in order to further increase productivity and evaluate their potential application. Moreover, the catalysts here reported were compared with other bimetallic Pd-Au samples supported on zirconia (Z), sulphated zirconia (SZ), ceria (Ce) and sulphated ceria (SCe) under identical reaction conditions in order to evaluate the effect of the support on metallic dispersion and morphology and the relevant effect on catalytic activity and selectivity.

2. Experimental

2.1 Materials

$ZrOCl_2$ (Fluka), $(NH_4)_2Ce(NO_3)_6$ (Sigma Aldrich), $(NH_4)_2SO_4$ (Merck), were used as received for sample synthesis. SiO_2 (Akzo) was used as received for catalysts preparation.

All kinetic tests were performed in anhydrous methanol (SeccoSolv, Merck, $[H_2O] < 0.005\%$). Commercial standard solutions of $Na_2S_2O_3$ (Fixanal [0.01], Hydranal-solvent E, and Hydranal-titrant 2E, all from Riedel-de Haen) were used for iodometric and Karl-Fischer titrations.

2.2. Catalysts preparation

Commercial silica (Akzo) was used as received for catalysts preparation (Si).

$Zr(OH)_4$ was prepared by precipitation from $ZrOCl_2$ at pH=10, aged under reflux conditions for 20 hours [44, 45], washed free from chloride ($AgNO_3$ test) and dried at 110 °C overnight. Part of this material was impregnated by incipient wetness method with ammonium sulphate, in amounts necessary to yield a nominal anion loading of 8% by weight. Sulphated (SZ) and not sulphated (Z) hydroxides were then calcined in flowing air (30 ml/min) at 650 °C for 4 hours.

Ceria support was synthesized by precipitation from $(NH_4)_2Ce(NO_3)_6$ by urea at 100 °C in aqueous solution [46]. The solution was continuously mixed and boiled for 6 h at 100 °C, the precipitate was

washed twice in boiling deionized water and dried at 110 °C overnight. Part of this material was impregnated by an incipient wetness method with $(NH_4)_2SO_4$ in amounts necessary to yield an 8% wt anion loading. Both impregnated (SCe) and not impregnated (Ce) supports were then calcined in flowing air (50 ml/min) at 650 °C for 3 hours.

As summarized in Scheme 2, metals were deposited on the five supports by incipient wetness (IW) co-impregnation of H_2PdCl_4 and $HAuCl_4$ aqueous solutions, followed by calcination at 500 °C in flowing air (30 ml/min) for 3 hours.

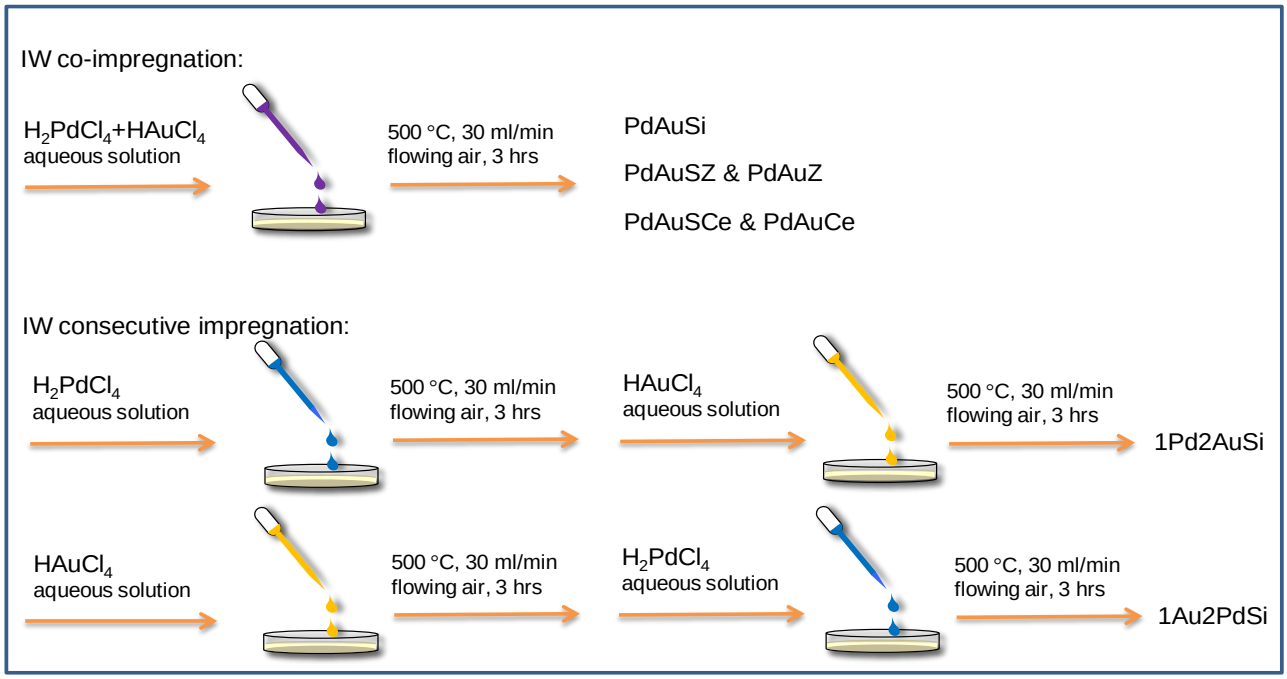

Scheme 2. Synthetic procedures followed to prepare the catalysts.

Moreover, SiO_2 was used as support for preparing other two bimetallic Pd-Au samples by consecutive impregnations. The amounts of precursors employed were calculated to yield theoretical metal contents of Pd 1.5wt% and Au 1.5wt% in the final catalyst.

In the former case, the sample (1Pd2AuSi) was prepared depositing firstly Pd and then Au. In particular, Pd was deposited on the support by incipient wetness impregnation of a H_2PdCl_4 aqueous solution, then the material was dried at 110 °C overnight and calcined at 500 °C in flowing air (30 ml/min) for 3 hours. In a second step, Au was introduced by impregnation of a $HAuCl_4$ aqueous solution. The sample obtained was then washed with NH_4Cl (0.25 M) [47], washed with distilled water, dried and calcined at 500 °C in flowing air (30 ml/min) for 3 hours.

The latter catalyst (1Au2PdSi) was prepared according to the previous procedure, but inverting the deposition order: first gold, then palladium by IW method. The sample was finally calcined under the same conditions reported above.

2.3. Characterization methods

Surface areas and pore size distributions were obtained from N_2 adsorption/desorption isotherms at -196 °C (using a Micromeritics ASAP 2000 analyser). Calcined samples (300 mg) were pre-treated at 300 °C for 2 hours under vacuum. The surface area was calculated from the N_2 adsorption isotherm by the BET equation, and the pore size distribution was determined by the BJH (Barrett-Joyner-Halenda) method [48]. The total pore volume was taken at $p/p_0 = 0.99$.

The actual metal loadings were determined by atomic absorption spectroscopy after microwave breakdown of the samples (100 mg).

The amount of sulphate was determined by ion exchange chromatography (IEC) after dissolution of the materials [49]. All sulphate concentrations were calculated as the average of two independent sample analyses, and each analysis included two chromatographic determinations.

Temperature programmed reduction (TPR) experiments were carried out in a lab-made equipment: samples (100 mg) were heated with a 10 °C/min ramp from 25 °C to 1000 °C in a 5% H_2/Ar reducing mixture (40 mL/min STP).

High-resolution transmission electron microscopy (HRTEM) analysis was performed by means of a JEOL JEM 3010-UHR microscope operating at 300 kV, equipped with a (2k × 2k)-pixel Gatan US1000 CCD camera and with an OXFORD INCA EDS instrument for atomic recognition via energy dispersive spectroscopy (EDS). The powdered samples were deposited on a copper grid covered with a lacey carbon film. A statistically representative number of particles was counted in order to obtain the Pd particle size distribution.

Diffuse reflectance UV–Vis-NIR (DR UV-Vis-NIR) spectra measurements were performed at room temperature on a Varian Cary 5000 spectrophotometer, working in the 190-2500 nm wavelength range. DR UV–Vis-NIR spectra are reported in the Kubelka-Munk function [$f(R\infty)=(1-R\infty)2/2R\infty$; $R\infty$=reflectance of an "infinitely thick" layer of the sample. The powders were hand milled in a agate mortar and placed in a cell with a quartz window, allowing to run the spectra in air.

2.4. Catalytic tests

Some catalytic tests were carried out at atmospheric pressure in a 20°C thermostatted glass reactor according to a previously described procedure [33, 43]. Mixing was carried out with a Teflon®-made rotor operating at 1000 rpm. Oxygen and hydrogen were bubbled by a gas diffuser directly into the liquid phase with a total flow of 50 ml/min in continuous. A gas mixture with the following composition was used: H_2:O_2 4:96 (non-explosive and lower limit for non-flammable mixture) [50].

The reaction medium was 100 ml of a 0.03 M H_2SO_4 methanolic solution and was pre-saturated with the gas mixture before catalyst (135 mg) introduction. Samples were pre-treated in situ first by H_2 (15 min - 30ml/min) and then by O_2 (15 min - 30 ml/min) flow (surface oxidation). During catalytic tests small aliquots of the liquid phase were sampled through a septum and used for water and hydrogen peroxide determination. Preliminary experiments showed that the system works in a strictly kinetic regime. H_2O_2 concentration was measured by iodometric titration, whereas water was determined by volumetric Karl–Fischer method. The water content in the reaction medium before catalyst addition was determined prior to each catalytic experiment. H_2O_2 selectivity at time t was calculated as follows:

$$S_{H_2O_2} = \frac{[H_2O_2]}{[H_2O_2]+[H_2O]}$$

High pressure catalytic tests were performed at 20°C using an autoclave with a nominal volume of 250 ml. The reaction medium was 100 ml of a 0.03 M H_2SO_4 methanolic solution. The water content in the reaction medium was determined prior to each catalytic experiment before catalyst (50 mg) introduction. Typically, the autoclave was loaded, purged three times with CO_2 (10 bar) and then filled with the reactants to give a total pressure of 10 bar. A gas mixture with the following composition was used: H_2 : O_2 : CO_2 = 3.6 : 7.2 : 89.2 (non-explosive and non-flammable mixture) [50]. Mixing was carried out with a Teflon®-made rotor operating at 1200 rpm. Experiments were carried out for 30 min. Water and hydrogen peroxide determination were measured as previously reported after each catalytic test.

3. Results and Discussion

3.1. PdAu bimetallic samples supported on silica

Commercial silica was used as support for preparing the three bimetallic Pd-Au samples by different procedures (Scheme 2). Pd and Au amounts on the final samples are reported in Table 1.

Interestingly, the gold amount is significantly lower than the theoretical one in the two catalysts prepared by consecutive impregnation. During the synthetic procedure washing with NH_4Cl was adopted after the impregnation step to stabilize small Au particles [47], a procedure whose efficacy was later found to be strongly pH dependent [51]. Similarly, the Pd amount on 1Pd2AuSi is the lowest, despite intermediate calcination, due to subsequent gold impregnation and washing.

The effect of the different preparation methods on the reaction was investigated. The catalytic tests were carried out in methanol, because this solvent has many advantages: (i) it helps H_2 solubility while avoiding the formation of peroxides, at variance with higher alcohols [41]; (ii) the use of methanol as a solvent allows water titration and therefore the determination of the process selectivity; (iii) most oxidation reactions involving H_2O_2 are carried out in organic solvents, often in methanol, thus the synthesis in this solvent could be an advantage avoiding separation and concentration costs.

Some catalytic tests were carried out at room temperature, atmospheric pressure, outside the explosion range, without halide addition, after a mild activation in oxygen, a process giving rise to Pd particle surface oxidation [33]. This pre-treatment is as follows: samples are reduced *in situ* by passing a pure hydrogen flow into the reaction medium, leading to a completely reduced catalyst. Then, pure oxygen is fed. Excess oxygen is then removed by passing pure nitrogen. The undiluted hydrogen/oxygen mixture used for the catalytic tests allows to maintain the sample surface oxidized [33], a condition that has proved advantageous for catalytic activity and selectivity. Moreover, we have performed catalytic tests in a 0.03 M H_2SO_4 methanolic solution. In fact, it's known that the use of acidic solutions (e.g., H_2SO_4 or HCl) promote the peroxide formation and stabilization [2], since in neutral solution H_2O_2 can easily decompose. We decided to use H_2SO_4 because chlorine ions could create problems of corrosion, of possible formation of dangerous Cl_2, of Pd leaching by complex formation with Cl^-.

The H_2O_2 concentration together with the selectivity trends for the different samples is shown in Figure 1, while both productivity and selectivity after 5 hours are reported in Table 1. Since all catalysts are bimetallic, the reported productivity was calculated with respect to the catalysts amount. The best catalytic results were obtained using the PdAuSi sample, indicating that the effect of gold addition to Pd in enhancing the yield of H_2O_2 is sensitive to the preparation method and the consequent Au amount. Such catalyst shows a linear increase in hydrogen peroxide formation with time and the highest and constant selectivity during 5 hours of reaction. In particular, PdAuSi allows achieving, already at atmospheric pressure, a H_2O_2 concentration over 100 mM and a H_2O_2 selectivity of 55%. A completely different behaviour was found for the two samples prepared by consecutive impregnations. The 1Pd2AuSi catalyst shows a linear profile in H_2O_2 concentration only for the first 2 hours of reaction, and then both productivity and selectivity slow down. This means that, beyond this point, H_2O_2 decomposition starts prevailing over H_2O_2 formation. The difference with respect to the PdAuSi sample is remarkable, since the H_2O_2 concentration is 60 mM instead of 100 mM under the same conditions. The H_2O_2 concentration profile for 1Au2PdSi catalyst is linear and even higher than that of PdAuSi. However, the

selectivity trend shows also a linear decrease and the value declines from 50 to 39 % for this sample. In this case the catalyst is very active for both H_2O_2 and H_2O formation.

These data confirm that the overall activity is mainly related to the amount of Pd present on the catalyst while Au amount is unimportant but at the same time they suggest that the preparation method plays an important role on selectivity.

Catalytic tests at higher pressures, still working outside the explosive region, at room temperature and without halide addition, have been also carried out for the two best catalysts (PdAuSi and 1Au2PdSi). CO_2 was used as a diluent inert gas because the explosive region for H_2/O_2 mixtures in CO_2 is much narrower than in other inert gases [41] and its acidity could help avoid hydrogen peroxide decomposition. Besides carbon dioxide is naturally abundant, relatively non-toxic and non-flammable [41, 52].

As reported in Figure 2, the productivity at 10 bar is much higher than at 1 bar by a higher than 10 times factor. This is true for all the prepared bimetallic samples and it is a confirmation of previous results obtained on different Pd based catalysts [53]. Moreover, the selectivity is only slightly lower than for the catalytic tests performed at 1 bar (Figure 2), even if the selectivity of the PdAuSi decreases to a less extend than 1Au2PdSi. Again, the PdAuSi catalyst is the best performing one under these reaction conditions, producing 12000 $mmolH_2O_2/g_{Me}h$ with a selectivity of 53%.

These results confirm that the catalytic performance is strongly dependent on the preparation method, which can induce different Pd-Au interactions and/or metal particle morphologies. Therefore, the samples were analyzed by TPR analyses in order to investigate the metal oxidation state in relation with the synthesis conditions and to identify possible interactions between palladium and gold. Figure 3 shows the TPR profiles for the PdAu bimetallic catalysts supported on silica.

All catalysts show a negative peak at about 70 °C, due to hydrogen evolution (mass spectrometry evidence) from β-hydride decomposition [54, 55], indicating the presence of Pd (II) species, already reducible at room temperature. In addition, a supplementary peak centered at about 150 °C is observed in the TPR pattern of the PdAuSi sample. This feature is not present in the TPR profiles of 1Pd2AuSi and 1Au2PdSi catalysts and it is related to the reduction of a PdAuO oxide-like phase [53]. This means that the samples prepared by consecutive impregnations contain only room temperature reducible PdO species. On the contrary, the PdAuSi sample shows both the Pd hydride decomposition peak, meaning that there is a palladium phase able to absorb hydrogen at ambient temperature, and a reduction peak at 150 °C, indicating the presence of a PdAuO. Such positive reduction peak is an indication of the enhanced stability of the oxidic phase for this catalyst

[53]. As will be discussed in Scheme 3, such enhanced stability of the oxidic phase is responsible for the higher catalytic performances. On the contrary, the presence of only reduced Pd particles can be related to the low selectivity of the 1Pd2AuSi and 1Au2PdSi catalysts.

HRTEM measurements combined with EDS analysis were performed on the PdAuSi catalyst to get more information on the composition and morphology of the supported metallic phase. Particles agglomerates with indented profile and with sizes 35-70 nm as well as a few small Pd particles with size around 2 nm have been observed (see section a of Figure 4). These aggregated particles are made by Pd, as confirmed by the EDS analysis reported in the Figure. Moreover, by doing the FFT (Fast Fourier Transform) of the image (inset), the 101 and 100 faces of tetragonal PdO [54] have been recognized, indicating the presence of PdO particles aggregates that, once reduced at room temperature, cause the negative TPR peak around 70 °C. At the same time, a large amount of big particles with size ranging from 30 nm up to 50 nm, roundly shaped and homogeneous in terms of phase contrast have been recognized. In this case, EDS reveals the presence of both Au and Pd in the composition, indicating that these species can be alloy particles, giving rise to the peak at 150 °C in the TPR profile of PdAuSi. A typical alloy particle with the respective EDS spectrum is shown in section b of Figure 4. Similar alloy particles were previously observed by HRTEM and XRD measurements on bimetallic catalysts supported on zirconia and prepared according to the same procedure [53].Finally, some very large gold particles with size in the 100-300 nm range have been also observed. To get more insight into the chemical composition of the bimetallic phase, the alloy Au/Pd ratio was calculated from the % Au and Pd amounts obtained by EDS analysis. We found that the Au/Pd ratio ranges between 0.04 and 0.09, indicating that the composition of the alloy particles is much richer in Pd.

We already proposed a possible reaction pathway for the formation of hydrogen peroxide on monometallic Pd catalysts [56]. Accordingly, oxygen can chemisorb with or without dissociation depending on the chemisorption sites that can be more or less energetic. In this context, the co-presence of gold can modify the Pd active sites by rendering them less energetic, i.e. able to chemisorb the oxygen molecule without dissociation, a necessary condition to give the desired H_2O_2 product. Our previous FTIR results on differently prepared Pd-Au/ZrO_2 catalysts evidenced that the active palladium sites are more easily oxidized as a consequence of the presence of a PdAu phase [51]. On the contrary, in the presence of more energetic Pd sites (defects, edges, corners, etc.) O_2 chemisorbs and dissociates leading to the formation of water. As an alternative view, the presence of gold could make dissociatively chemisorbed oxygen atoms strongly bound to Pd (as indicated by the TPR band at 170°C) reducing its capacity to produce water, thereby indirectly increasing hydrogen peroxide selectivity.

The morphological properties of PdAuSi (the most selective catalyst) seem to fulfill the need of less energetic sites, for good selectivity. In fact, oxidized PdAuO less energetic sites exposed at the surface of the alloy particles observed on this sample are able to produce hydrogen peroxide by activating O_2 without dissociating it, as represented in Scheme 3. Therefore, the presence of reduced Pd particles (not containing PdAuO sites) can explain the low selectivity of the 1Pd2AuSi and 1Au2PdSi catalysts, according to Scheme 3.

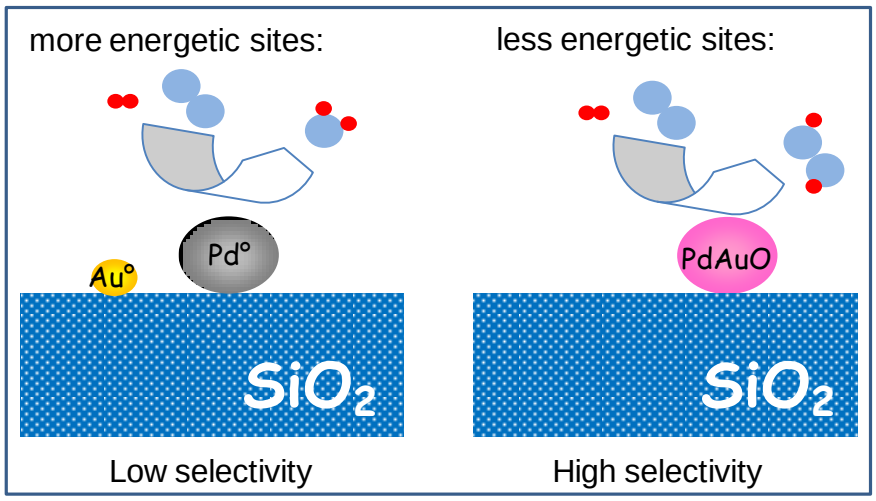

Scheme 3. Nature of the Pd and Au active sites on the different bimetallic catalysts.

These findings pointed out that the choice of the preparation method, i.e. IW co-impregnation rather than IW consecutive impregnations, is crucial for determining the morphology of the metallic active phase which strongly affects the catalytic performance in terms of both conversion and selectivity.

3.2 Co-impregnated PdAu catalysts on different supports

In order to evaluate how the nature of the support influences the catalytic activity, a comparison among bimetallic samples prepared by the same synthetic route (simultaneous co-impregnation with palladium and gold aqueous solutions) on different oxides has been performed.

Since H_2O_2 is more stable under acidic conditions, an acidic support may prove useful, in principle, for the direct synthesis of H_2O_2. In this respect silica, with its moderate acidic properties, is a suitable choice. Other advantages of silica are non-toxicity, good availability and low cost. Similarly, the intrinsic chemical and physical characteristics, that can be adjusted by choosing different precursors and synthesis conditions, render zirconia a promising support. Finally, ceria is characterized by a high oxygen storage capacity and reducibility and these properties may be exploited in a reaction in which oxygen activation plays a fundamental role.

It is known [57] that the surface acidity/basicity of zirconia can be controlled by addition of different dopants, SO_4^{2-} being the most investigated one. We have therefore investigated sulphated zirconia and sulphated ceria as supports for the PdAu bimetallic samples.

A comparison of the catalytic behaviours is shown in Figure 5, while the corresponding data are reported in Table 2. All catalysts show a constant H_2O_2 formation as well as constant selectivity over the whole duration of the test (360 min). The productivity after 5 hours follows the order: PdAuSi ≈ PdAuSZ > PdAuZ >> PdAuCe ≈ PdAuSCe. The PdAuSZ sample shows the highest selectivity (constant at 61%) and the following selectivity trend was observed: PdAuSZ > PdAuSi > PdAuSCe ≈ PdAuCe ≈ PdAuZ.

The data indicate that the acidity of the support is indeed an important practical issue as both conversion and selectivity increase. Moreover, the sulphating procedure has a promotion effect on the catalytic performance when applied to zirconia, while it is unimportant when applied to ceria. We have already demonstrated [33] that sulphated zirconia is an excellent support for this reaction with monometallic Pd-based catalysts, performing better than plain zirconia.

Catalytic tests at higher pressures, still working outside the explosive region, at room temperature with CO_2 as a diluent inert gas and without halide addition, have been also carried out with the best performing samples. As reported in Figure 7, the productivity at 10 bar is much higher than at 1 bar for all examined catalysts by a factor even higher than 10 times. This is true for all PdAu samples prepared and it is a confirmation of our previous results obtained on different Pd based catalysts [58]. Moreover, the selectivity is similar for the three samples when working at 10 bar.

In the present work the ZrO_2 and CeO_2 supports were impregnated before calcination with sulphate amounts necessary to yield 8% wt anion loading. In calcined (650 °C) sulphated zirconia samples the final amount of sulphates is about 4% wt, a typical value for these catalysts [59] while for ceria supported samples, the values are higher, about 7% wt. Palladium and gold amounts are reported in Table 2. N_2 physisorption analysis has been carried out in order to determine the surface area and pore size distribution of the samples. In this investigation, the choice of a mesoporous material as support is very important, since the presence of micropores could cause mass transfer problems, while a low surface area would not allow a good dispersion of the Pd and Au active phases. The N_2 physisorption isotherms for the five samples are shown in Figure 6, together with their BJH (Barrett-Joyner-Halenda) pore size distributions (see insert). A type IV isotherm with hysteresis loop typical of mesoporous materials is observed for all the catalysts. The sample supported on silica shows a surface area of 330 m^2/g and a mean pore diameter of about 9 nm.

Surface area of the PdAuSZ sample is about 142 m^2/g and the mean pore size around 9.8 nm, similarly to previous works [59].

As to the PdAuZ sample, a relatively low surface area (< 60 m^2/g) and a mean pore size around 20 nm can be calculated, in agreement with previous works for zirconia catalysts prepared by this method [33]. Also ceria samples display type IV isotherms with hysteresis loops typical of mesoporous materials. However, in ceria samples sulphates do not prevent structure collapse and pore wall thickening. At variance with zirconia, the sulphated material has a very low surface area (< 30 m^2/g), even lower than the plain ceria support (< 50 m^2/g). No correlation between conversion/selectivity and specific surface area (SSA) has been found. Therefore, similarly to the silica supported samples reported above, the differences in the catalytic performance may be explained by looking at the morphology of co-impregnated Pd and Au phases. HRTEM measurements were carried out on the catalysts supported on zirconia, sulphated zirconia and sulphated ceria. The main findings of this characterisation are shown in Figure 8, where the HRTEM representative images of the three samples are compared. Here we focus on the metallic phase, however for a more comprehensive description of the results see also references [33] and [53].

The PdAuZ sample exhibits small Pd particles of 2 nm size (see inset) and a large amount of roundish big particles with size in the 100-300 nm interval (section a of Figure 8). The EDS analysis confirmed that the composition of the latter species is bimetallic and the Au/Pd ratio varies between about 3 and 7, indicating that the alloy particles are richer in Au. The presence of very large particles containing mainly Au can be explained by considering that the co-impregnation procedure followed during the preparation of the sample is not a suitable method to obtain highly dispersed Au nanoparticles. As to PdAuSZ, small Pd particles with size around 3 nm (shown in the inset) have been observed as well as many large particles (section b of Figure 8). The sulphated ceria-supported catalyst revealed only very small metallic particles with average diameter of 1.5 nm [33] while no separate large metallic particles have been detected in this case.

DR UV-Vis-NIR measurements were undertaken to fully understand the nature of the Pd-Au phase, the spectra of the as prepared samples are reported in Figure 9. All spectra of the as prepared bimetallic samples show an exponentially increasing absorbance towards higher energy, that can be a consequence of the occurrence of interband transitions related to the PdAu particles formation [60]. HRTEM analyses evidenced a very heterogeneous metal dispersion on PdAuZ, PdAuSZ and PdAuSi. In particular, due to the preparation method, small monometallic Pd particles as well as very big bimetallic alloy particles, whose composition depends on the nature of the support, have also been observed. No UV-Vis plasmonic absorption band of gold was detected, confirming that

there is no separate formation of pure Au nanoparticles or, alternatively, only big gold agglomerates without small nanoparticles, able to give the plasmonic band, are available on the PdAu samples supported on silica, zirconia and sulphated zirconia. However, an absorption band at about 460 nm due to the Pd^{2+} d-d transition [61] is well evident in the case of PdAuZ, indicating that small PdO nanoparticles are present on this sample (see the inset of Figure 8b). On the contrary, on the other samples, the Pd^{2+} d-d transition is covered by a large absorption. A separate comment is needed for the PdAuSCe catalyst, where only small nanoparticles have been detected (Section c of Figure 8). The monotonous absorption is observed also in this case, suggesting a bimetallic nature of all observed nanoparticles with no separate formation of pure Au nanoparticles.

The HRTEM characterisation as well as the results coming from DR UV-Vis-NIR spectra suggest that, although the preparation method is the same, the morphology of the bimetallic phase is strongly related to the nature of the support. It could be hypothesized that acid properties play a role in determining the final morphology of the bimetallic PdAu catalysts. Pd nanoparticles together with large alloy particles are present on silica and on sulphated and pure zirconia. These bimetallic particles are richer in Pd when supported on silica and richer in Au in the case of both zirconia catalysts, although this does not appear to influence significantly the catalytic behaviour. On these samples, the PdAuO phase guarantees the presence of less energetic sites, able to activate oxygen without dissociation, hence obtaining good selectivity. On the contrary, only small alloy particles have been observed on sulphated ceria, i.e. the most basic support. These small bimetallic nanoparticles are expected to expose mainly edges and corners, therefore resulting in the presence of more energetic sites that lead to the formation of water. Hutchings and coworkers recently reported a marked synergistic effect between Au and Pd in H_2O_2 formation over bimetallic catalysts supported on carbon, TiO_2, Al_2O_3 and Fe_2O_3 whereas CeO_2-based catalyst show no synergy between Au and Pd [62], in agreement with our findings. Similarly to the indications of the present work these authors suggested that the origin of this undesired effect was most likely due to lack of alloy formation under the reaction conditions used. Once again these results emphasize the fundamental role of the support and (as demonstrated in the present work) of the preparation method in determining the right particle morphology and the appropriate electron density on Pd necessary to maximize H_2O_2 selectivity.

4. Conclusions

Bimetallic Pd-Au catalyst supported on silica were prepared by IW co-impregnation and consecutive IW impregnations. It has been found that the effect of gold addition to Pd in enhancing the yield of H_2O_2 is sensitive to the preparation method. In particular, the best catalytic results in

terms of both productivity and selectivity were obtained using the co-impregnated PdAuSi sample, according to the trend: PdAuSi > 1Au2PdSi > 1Pd2AuSi. The HRTEM and TPR findings put in evidence that the choice of the preparation method, i.e. IW co-impregnation rather than IW consecutive impregnations, is crucial for determining the morphology of the metallic active phase which strongly affects the catalytic performances in terms of both conversion and selectivity. The presence of a PdAuO phase able to guarantee the availability of less energetic sites necessary to activate the oxygen molecule without dissociating it, can explain the catalytic performance of PdAuSi.

In addition, the PdAu catalysts prepared by IW co-impregnation on different supports have been compared in the direct synthesis of hydrogen peroxide. The productivity follows the trend: PdAuSi ≈ PdAuSZ > PdAuZ >> PdAuCe ≈ PdAuSCe. The presence of PdAu alloy particles has been observed on the samples and the characterization results indicate that there is an effect of the acidity of the support on both morphology and size of the bimetallic phase. In particular, the more acidic is the support, the larger is the size. However, basing on HRTEM and DR UV-Vis-NIR spectroscopy, only PdAuSi, PdAuSZ and PdAuZ contain bimetallic particles exposing the active less energetic sites. In contrast, the small bimetallic nanoparticles observed on ceria expose only more energetic sites that lead to the formation of water.

5. Acknowledgements

We thank Mrs.Tania Fantinel for technical assistance. Financial support to this work by MIUR (Rome) is gratefully acknowledged.

Tables and figures captions:

Table 1. Metal loading of bimetallic catalysts on silica and their catalytic results at atmospheric pressure.

Table 2. Characterizations of bimetallic catalysts on different supports and their catalytic results at atmospheric pressure.

Figure 1. H_2O_2 production and selectivity at atmospheric pressure with PdAuSi (●), 1Pd2AuSi (▲), 1Au2PdSi (□).

Figure 2. Comparison between H_2O_2 productivity and selectivity (after 30 min of reaction) for H_2O_2 direct synthesis performed at 1 bar and 10 bar.

Figure 3. TPR analyses of bimetallic catalysts supported on silica.

Figure 4. HRTEM representative images with EDS analyses of PdAuSi: a Pd particles agglomerate and relative EDS spectrum (section a), FFT of the image (inset) and an alloy particle and respective EDS spectrum (section b). Instrumental magnification: 300000X and 400000X, respectively.

Figure 5. H_2O_2 production and selectivity at atmospheric pressure with PdAuSi (●), PdAuZ (▼), PdAuSZ (○), PdAuCe (■), PdAuSCe (□).

Figure 6. N_2 physisorption isotherms of catalysts and (inset) their BJH pore size distributions. PdAuSi (●), PdAuZ (▼), PdAuSZ (○), PdAuCe (■), PdAuSCe (□).

Figure 7. Comparison of catalytic results (after 30 minutes) at different pressure.

Figure 8. HRTEM images of PdAuZ (section a), PdAuSZ (section b) and PdAuSCe (section c). Instrumental magnification: 100000X and 500000X (section a); 100000X and 300000X (section b) and 500000X (section c), respectively.

Figure 9. DRUV-Vis spectra of as prepared PdAuZ (blue curve), PdAuSZ (green curve), PdAuSi (red curve) and PdAuCe (magenta curve).

Table 1. Metal loading of bimetallic catalysts on silica and their catalytic results at atmospheric pressure.

sample	%Pd (wt%)	%Au (wt%)	Productivity after 5 h ($mmol_{H2O2}/g_{cat}h$)	Selectivity after 5 h (%)
PdAuSi	1.7	1.5	13.6	55
1Pd2AuSi	1.1	0.1	8.9	33
1Au2PdSi	1.7	0.1	14.1	39

Table 2. Characterizations of bimetallic catalysts on different supports and their catalytic results at atmospheric pressure.

sample	Surface area (±1 m^2/g) (m^2/g)	Pd found (wt%)	Au found (wt%)	Productivity after 5 h ($mmol_{H2O2}/g_{cat}h$)	Selectivity after 5 h (%)
PdAuSi	331	1.7	1.5	13.6	55
PdAuZ	61	1.2	0.9	12.2	40
PdAuSZ	130	1.2	0.9	13.6	61
PdAuCe	53	1.3	1.1	7.2	42
PdAuSCe	30	1.0	1.1	7.1	44

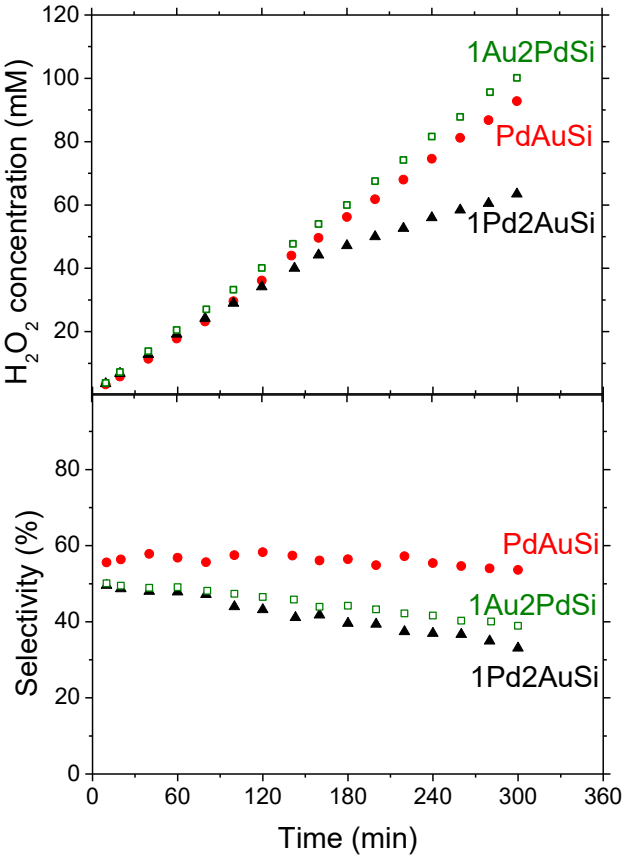

Figure 1. H_2O_2 production and selectivity at atmospheric pressure with PdAuSi (●), 1Pd2AuSi (▲), 1Au2PdSi (□).

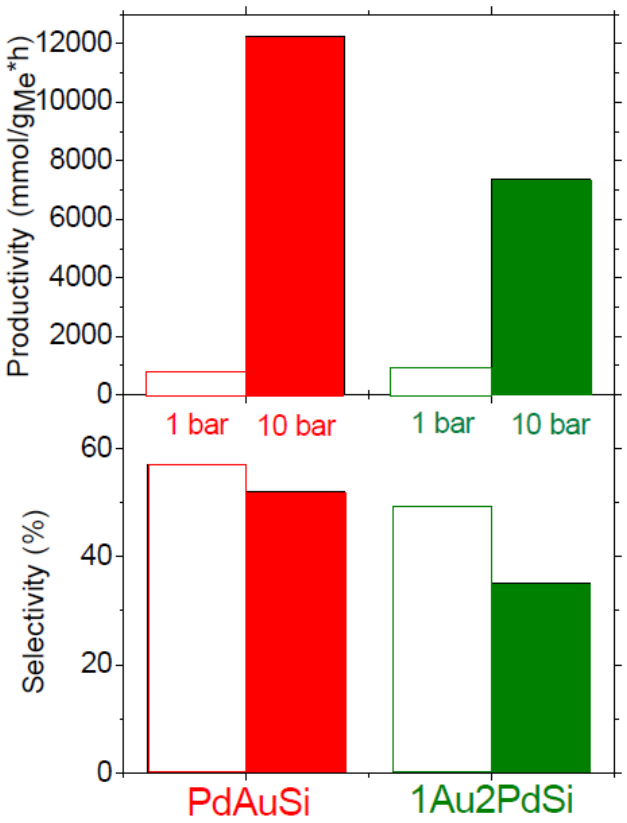

Figure 2. Comparison between H_2O_2 productivity and selectivity (after 30 min of reaction) for H_2O_2 direct synthesis performed at 1 bar and 10 bar.

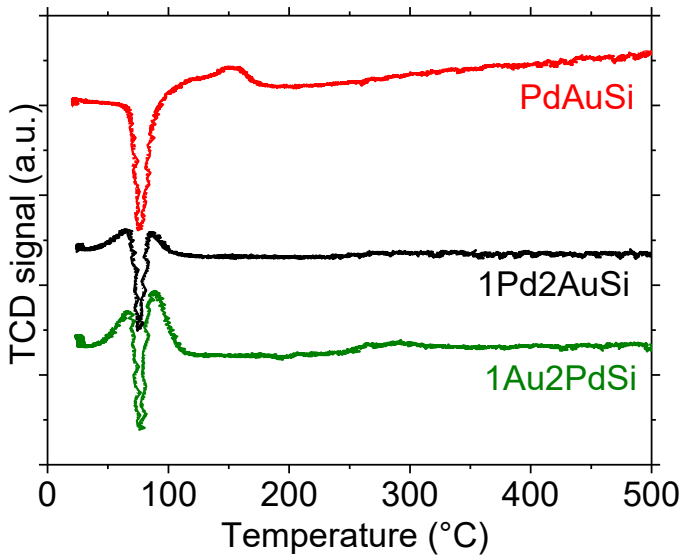

Figure 3. TPR analyses of bimetallic catalysts supported on silica.

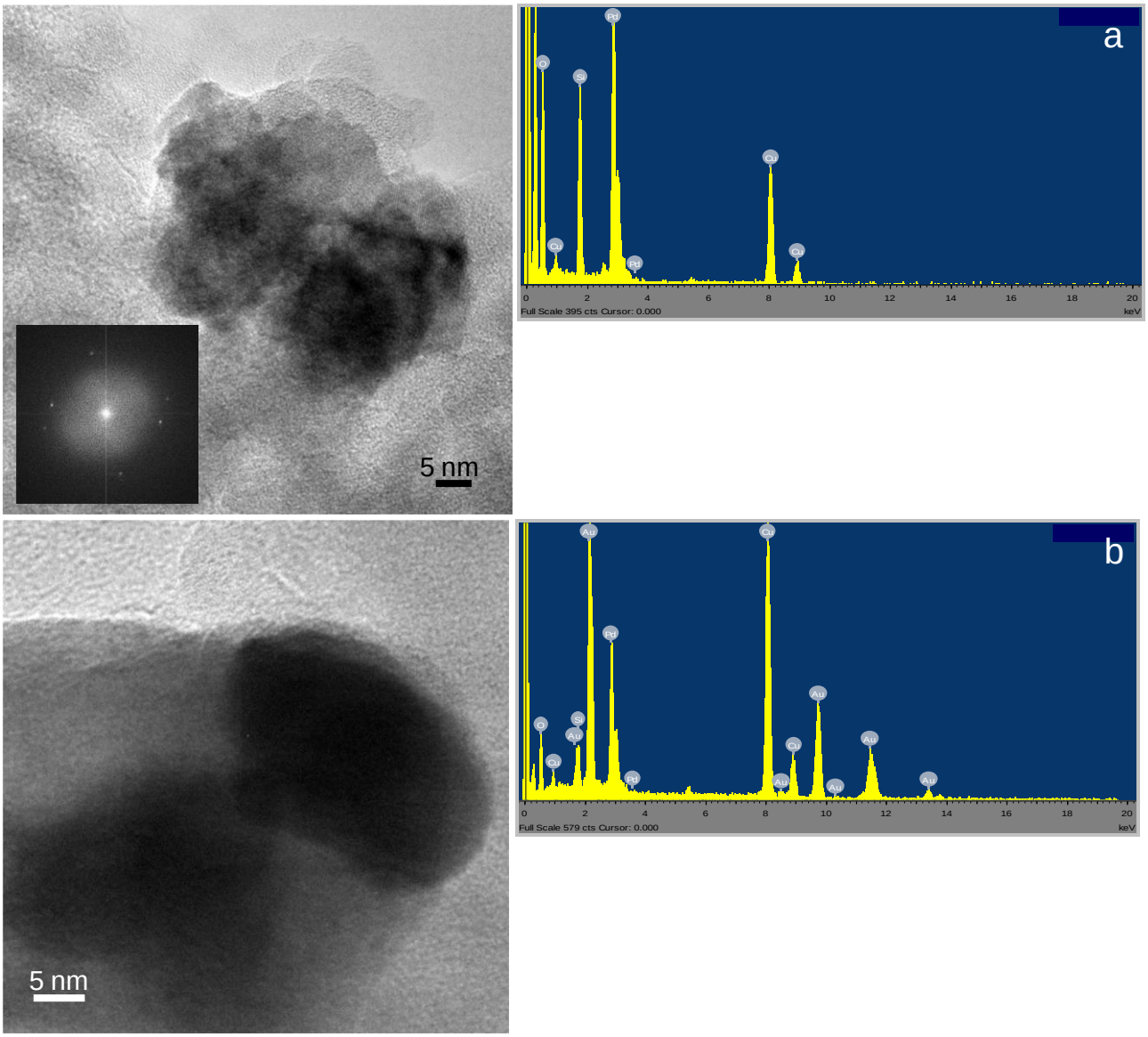

Figure 4. HRTEM representative images with EDS analyses of PdAuSi: a Pd particles agglomerate and relative EDS spectrum (section a), FFT of the image (inset) and an alloy particle and respective EDS spectrum (section b). Instrumental magnification: 300000X and 400000X, respectively.

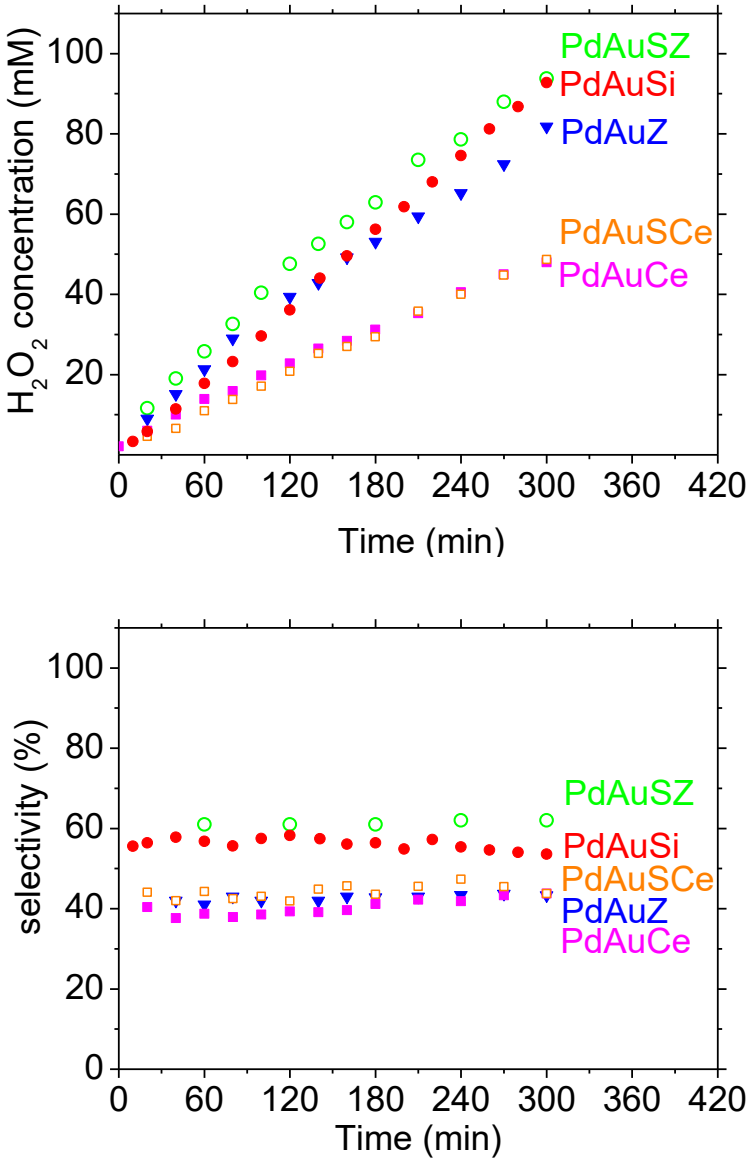

Figure 5. H_2O_2 production and selectivity at atmospheric pressure with PdAuSi (●), PdAuZ (▼), PdAuSZ (○), PdAuCe (■), PdAuSCe (□).

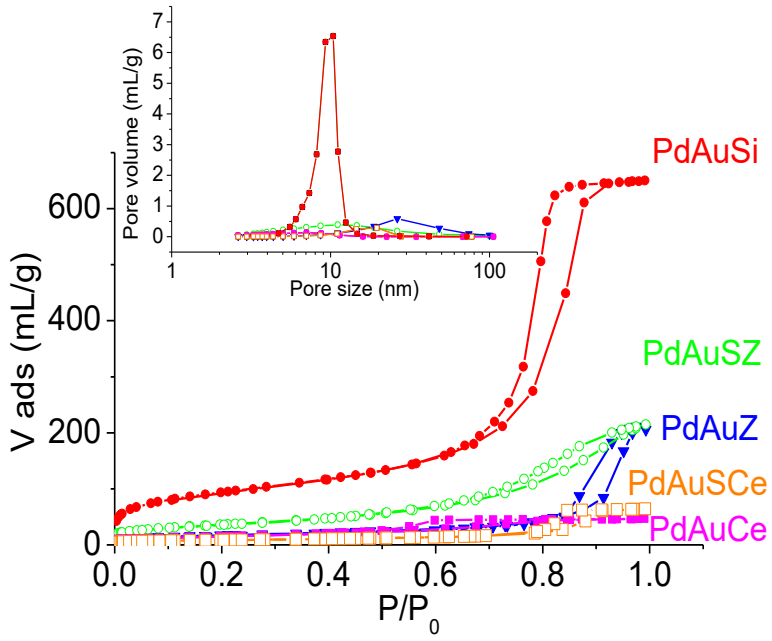

Figure 6. N_2 physisorption isotherms of catalysts and (inset) their BJH pore size distributions. PdAuSi (●), PdAuZ (▼), PdAuSZ (○), PdAuCe (■), PdAuSCe (□).

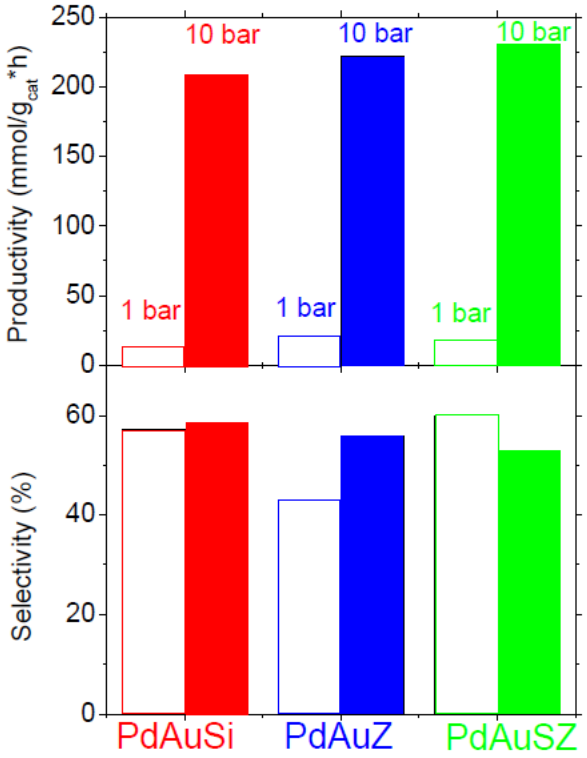

Figure 7. Comparison of catalytic results (after 30 minutes) at different pressure.

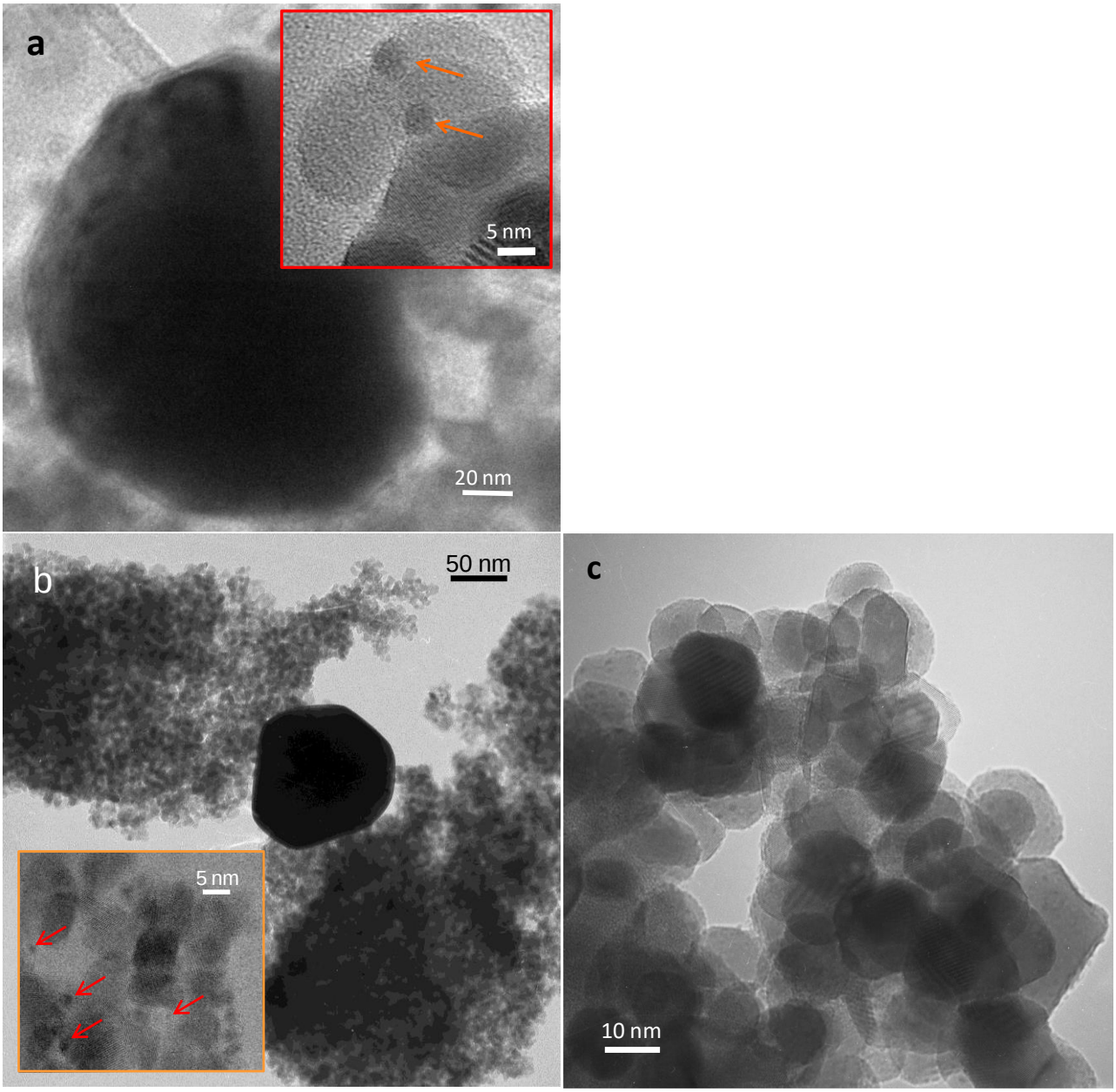

Figure 8. HRTEM images of PdAuZ (section a), PdAuSZ (section b) and PdAuSCe (section c). Instrumental magnification: 100000X and 500000X (section a); 100000X and 300000X (section b) and 500000X (section c), respectively.

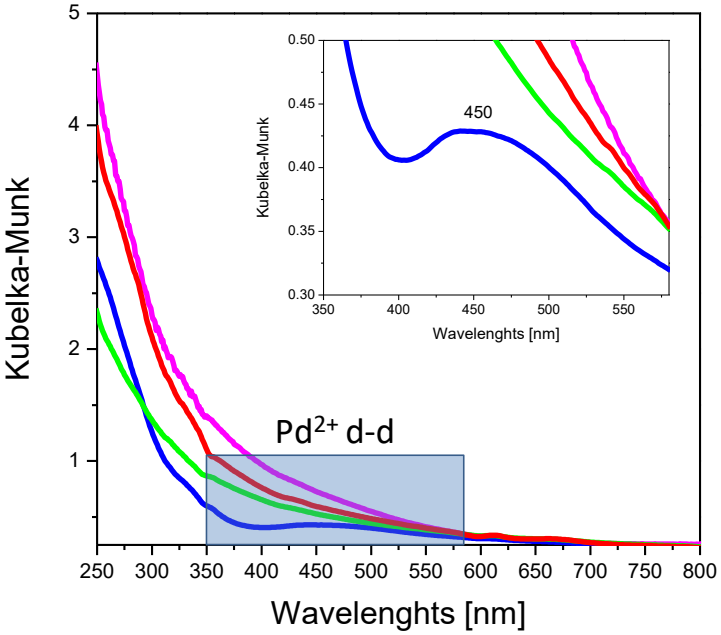

Figure 9. DRUV-Vis spectra of as prepared PdAuZ (blue curve), PdAuSZ (green curve), PdAuSi (red curve) and PdAuCe (magenta curve).

6. References

[1] (a) C.W. Jones, Applications of hydrogen peroxide and derivates, Clean technology monographs, Royal Society of Chemistry, Cambridge, 1999. (b) G. Strukul (Ed.), Catalytic Oxidations with Hydrogen Peroxide as Oxidant, Kluwer, Dordrecht 1992.
[2] G. Strukul, A. Scarso, "Environmentally Benign Oxidants", in Liquid Phase Oxidation via Heterogeneous Catalysis, M. G. Clerici, O. Kholdeeva Eds., Wiley, London 2013, pp 1-20.
[3] (a) B. Notari, Adv. Catal. 41 (1996) 253-334. (b) A. Scarso, G. Strukul, "Catalytic Oxidation Processes", in Comprehensive Inorganic Chemistry, vol. 6, J. Reedijk, K. Poeppelmeier Eds in Chief, Elsevier: Oxford 2013, ch. 6.08, pp. 177-221.
[4] H.-J. Riedl and G. Pfleiderer, US 2215883 (1940).
[5] S. Abate, G. Centi, S. Perathoner, S. Melada, F. Pinna, G. Strukul, Top. Catal. 38 (2006) 181-193.
[6] L.W. Gosser, US 4681751 (1987).
[7] L.W. Gosser, J.T. Schwartz, US 4772485 (1988).
[8] J. Van Weynbergh, J.-P. Schoebrechts, US 5447706 (1995).
[9] B. Bertsch-Frank, I. Hemme, S. Katusic, J. Rollmann, US 6387364 (2002).
[10] G. Paparatto, R. D'Aloisio, G. De Alberti, R. Buzzoni, US 6630118 (2003).
[11] K.M. Vanden Bussche, S.F. Abdo, A.R. Oroskar, US 6713036 (2004).
[12] R. Burch, P.R. Ellis, Appl. Catal. B-Environ. 42 (2003) 203-211.
[13] V.R. Choudhary, P. Jana, J. Catal. 246 (2007) 434-439.
[14] C. Samanta, V.R. Choudhary, Catal. Commun. 8 (2007) 2222-2228.
[15] A. Herzing, A. F. Carley, J. Edwards, G.J. Hutchings, C.J. Kiely, Chem. Mater. 20 (2008) 1492-1501.
[16] J.K. Edwards, A. Thomas, B. Solsona, P. Landon, A.F. Carley, G. Hutchings, Catal. Today 122 (2007) 397-402.
[17] D. Hancu, E.J. Beckman, Green Chem. 3 (2001) 80-86.
[18] Q. Liu, J.H. Lunsford, J. Catal. 239 (2006) 237-243.
[19] P. Biasi, F. Menegazzo, F. Pinna, K.Eranen, P.Canu, T. Salmi, Ind. Eng. Chem. Res. 49 (2010) 10627-10632.
[20] P. Biasi, F. Menegazzo, F. Pinna, K.Eranen, T. Salmi, P.Canu, Chem.Eng. J. 176-177 (2011) 172-177.
[21] N. Gemo, P. Biasi, P.Canu, F. Menegazzo, F. Pinna, A. Samikannu, K. Kordas, T. Salmi, Top. Catal. 56 (2013) 540-549.
[22] P. Biasi, F. Menegazzo, P.Canu, F. Pinna, T. Salmi, Ind. Eng. Chem. Res. (2013) doi: ipdf/10.1021/ie4011782.
[23] Q. Liu, K. Gath, J.C. Bauer, R. E. Schaak, J.H. Lunsford, Catal. Lett. 132 (2009) 342-348.
[24] J. Edwards, B. Solsona, E. Ntainjua, A.F. Carley, A. Herzing, C. Kiely, G. Hutchings, Science 323 (2009) 1037-1041.
[25] F. Menegazzo, M. Signoretto, G. Frison, F. Pinna, G. Strukul, M. Manzoli, F. Boccuzzi, J. Catal. 290 (2012) 143-150.
[26] P. Biasi, P.Canu, F. Menegazzo, F. Pinna, T. Salmi, Ind. Eng. Chem. Res. 51 (2012) 8883-8889.
[27] T.A. Pospelova, N.I. Kobozev Russ. J. Phys. Chem. 35 (1961) 262-265.
[28] J.H. Lunsford, J. Catal. 216 (2003) 455-460.
[29] J.M. Campos-Martin, G. Blanco-Brieva, J.L.G. Fierro, Angew. Chem. 118 (2006) 7116-7139.
[30] J. A. Rodriguez, Prog. Surf. Sci. 81 (2006) 141-189.
[31] G. Li, J.K. Edwards, A.F. Carley, G. J. Hutchings, Catal. Commun. 8 (2007) 247-250.
[32] P. Landon, P.J. Collier, A.J. Papworth, C.J. Kiely, G.J. Hutchings, Chem. Commun. (2002) 2058-2059.

[33] F. Menegazzo, P. Burti, M. Signoretto, M. Manzoli, S. Vankova, F. Boccuzzi, F. Pinna, G. Strukul, J. Catal. 257 (2008) 369-381.
[34] G.Luft, U. Luckhoff, Chem. Eng. Technol. 66 (1994) 187-189.
[35] S. Abate, S. Melada, G. Centi, S. Perathoner, F. Pinna, G. Strukul, Catal. Today 117 (2006) 193-198.
[36] V.R. Choudhary, C. Samanta, T.V. Choudhary, Appl. Catal. A 308 (2006) 128-133.
[37] Q. Liu, J. C. Bauer, R.E. Schaak, J.H. Lunsford, Appl. Catal. A 339 (2008) 130-136.
[38] M. Haruta, T. Kobayashi, H. Sano, N. Yamada, Chem. Lett. (1987) 405-408.
[39] M. Haruta, N. Yamada, T. Kobayachi, S. Iijima, J. Catal. 115 (1989) 301-309.
[40] D. Andreeva, V. Idakiev, T.Tabakova, A. Andreev, J. Catal. 158 (1996) 354-355.
[41] J.K. Edwards, B. Solsona, P. Landon, A.F. Carley, A. Herzing, C. Kiely, G. Hutchings, J. Catal. 236 (2005) 69-79.
[42] N.S. Patil, B.S. Uphade, D.G. McCulloh, S.K. Bhargava, V.R. Choudhary, Cat. Comm. 5 (2004) 681-685.
[43] G. Bernardotto, F. Menegazzo, F. Pinna, M. Signoretto, G. Cruciani, G. Strukul, Appl. Catal. A: General 358 (2009) 129-135.
[44] S. Melada, M. Signoretto, F. Somma, F. Pinna, G. Cerrato, G. Meligrana, C. Morterra, Catal. Lett. 94 (2004) 193-198.
[45] M. Signoretto, S. Melada, F. Pinna, S. Polizzi, G. Cerrato, C. Morterra, Micr. Mes. Mater. 81 (2005) 19-29.
[46] L. Kundakovic, M. Flytzani-Stephanopoulos, J. Catal. 179 (1998) 203-221.
[47] L. Delannoy, N. El Hassan, A. Musi, N. N. Le To, J. Krafft, C. Louis, J. Phys. Chem. B 110 (2006) 22471-22478.
[48] S.J. Gregg, K.S.W. Sing, Adsorption, Surface Area and Porosity – 2nd ed., Academic Press, 1982, p. 111.
[49] C. Sarzanini, G. Sacchero, F. Pinna, M. Signoretto, G. Cerrato, C. Morterra, J. Mater. Chem. 5 (1995) 353-360.
[50] B. Lewis, G. von Elbe "Combustion, Flames and Explosion of Gases", Academic Press, New York and London, 1961.
[51] F. Somodi, I. Borbath, M. Hegedus, A. Tompos, I. Sajo, A. Szegedi, S. Rojas, J. L. G. Fierro, J. Margitfalvi, Appl. Catal. A 347 (2008) 216-222.
[52] E. J. Beckman, Green Chem. 5 (2003) 332-336.
[53] F. Menegazzo, M. Signoretto, M. Manzoli, F. Boccuzzi, G. Cruciani, F. Pinna, G. Strukul, J. Catal. 268 (2009) 122-130.
[54] Powder Diffraction File (PDF) number 00-006-0515.
W. Palczewska, in: “Hydrogen Effects in Catalysis” Z. Paal, P.G. Menon (Eds.), Dekker, New York, 1988, p. 373.
[55] Z. Karpinski, Adv. Catal. 37 (1990) 45-100.
[56] S. Abate, G. Centi, S. Melada, S. Perathoner, F. Pinna, G. Strukul, Catal. Today 104 (2005) 323-328.
[57] X. Song and A. Sayari, Catal. Rev.-Sci. Eng. 38 (1996) 329-412.
[58] E. Ghedini, F. Menegazzo, M. Signoretto, M. Manzoli, F. Pinna, G. Strukul, J. Catal. 273 (2010) 266-273.
[59] C. Morterra, G. Cerrato, F. Pinna, M. Signoretto, J. Catal. 157 (1995) 109-123.
[60] P. Dash, N.A. Dehm, R.W.J. Scott, J. Molec. Catal. A: Chemical, 286 (2008) 114-119, and references therein.
[61] G.P. Osorio, S.F. Moyado, V. Petranovskii, A. Simakov, Catal. Letters, 110 (2006) 53-60, and references therein.
[62] E.N. Ntainjua, M. Piccinini, J.C. Pritchard, J.K. Edwards, A.F. Carley, C.J. Kiely, G.J. Hutchings, Catal. Today, 178 (2011) 47-50.